Propagation and Damping of Two-Fluid Magnetohydrodynamic Waves in Stratified Solar Atmosphere

Yong-Jian Jin(金勇剑)[1**], Hui-Nan Zheng(郑惠南)[1,2], Zhen-Peng Su(苏振鹏) [1,2]

[1]*CAS Key Laboratory of Geospace Environment, Department of Geophysics and Planetary Sciences, University of Science and Technology of China, Hefei 230026*

[2]*Collaborative Innovation Center of Astronautical Science and Technology, University of Science and Technology of China, Hefei 230026*

(Received 19 April 2018)

An extreme ultra-violet (EUV) wave is characterized as a bright pulse that has emanated from the solar eruption source and can propagate globally in the solar corona. According to one leading theory, the EUV wave is a fast magnetoacoustic wave, as the coronal counterpart of the Moreton wave in the chromosphere. However, previous observations have shown that the EUV wave differs significantly from the Moreton wave in both velocity and lifetime. To reconcile these differences, here we analyze the wave characteristics of a two-fluid MHD model in the stratified solar atmosphere with a height-dependent ionization rate. It is found that the collision between neutral and ionized fluids is able to attenuate the wave amplitude, while causing a slight change in its propagation velocity. Because the chromosphere has the lower ionization rate and the stronger magnetic fields than the corona, the velocity of the Moreton wave is much higher than that of the EUV wave. In contrast to the Moreton waves damped strongly by the collision between neutral and ionized fluids, the EUV wave in the fully ionized corona is able to propagate globally on a time scale of several hours. Our results support the previous theory that fast magnetoacoustic waves account for both EUV and Moreteon waves in the different layers of the solar atmosphere.

PACS: 52.30.Cv, 52.30.Ex, 96.60.−j DOI: 10.1088/0256-307X/35/7/075201

Extreme ultra-violet (EUV) waves, also known as exteme-ultraviolet image telescope (EIT) waves, were first directly observed by an EIT onboard the solar and heliospheric observatory (SOHO).[1,2] They are characterized as bright pulses emanated from the solar eruption sources and can propagate globally in the solar corona.[3−5] Understanding the physical nature of EUV waves which has been controversial for almost 20 years is meaningful, such as coronal seismology uses observations of EUV waves propagating through the corona to estimate the rigorous coronal parameters like magnetic field strength, temperature, and density.[6,7] Two classes of physical processes have been proposed to explain the nature of EUV waves:[5,8,9] non-waves and waves. In the non-wave models, EUV waves are interpreted as pseudo-waves from the coronal magnetic-field reconfiguration during the coronal mass eruptions (CMEs).[10,11] The transient brightening is considered to be a result of the expanding of CME flux rope in the corona.[11,12] In the wave models, EUV waves are considered as the coronal counterpart of the Moreton waves propagating in the chromosphere.[13,14] They are interpreted as large-scale fast-mode magnetohydrodynamic (MHD) waves.[5,15−18] However, two significant differences between EUV and the Moreton waves have been reported:[5,8,9,18−25] (1) the velocities of EUV waves (200–500 km·s^{-1}) are much lower than those of the Moreton waves (500–2500 km·s^{-1});[5,8,26,27] (2) EUV waves (hours) have much longer lifetime than the Moreton waves (minutes).[4,5,8,24,26,27] In addition, some works treat the EUV waves as slow-mode waves or solitons.[28,29] A comprehensive overview of the observational and theoretical aspects of global coronal waves can be found in several recent reviews.[5,8,14,30,31]

To reconcile the differences between EUV and the Moreton waves, in this Letter we study the characteristics of MHD waves in the stratified solar atmosphere with a height-dependent ionization rate. The two-fluid MHD model for the partly ionized plasma can be written as[22,32−35]

$$\frac{\partial n_{\rm I}}{\partial t}+\nabla\cdot(n_{\rm I}\boldsymbol{u}_{\rm I})=0, \tag{1}$$

$$\frac{\partial p_{\rm I}}{\partial t}+\boldsymbol{u}_{\rm I}\cdot\nabla p_{\rm I}+\gamma p_{\rm I}\nabla\cdot\boldsymbol{u}_{\rm I}=0, \tag{2}$$

$$\frac{\partial \boldsymbol{u}_{\rm I}}{\partial t}+\boldsymbol{u}_{\rm I}\cdot\nabla\boldsymbol{u}_{\rm I}+\frac{1}{n_{\rm I}m_{\rm I}}\nabla p_{\rm I}-\boldsymbol{g}=\nu(\boldsymbol{u}_{\rm II}-\boldsymbol{u}_{\rm I}), \tag{3}$$

$$\frac{\partial n_{\rm II}}{\partial t}+\nabla\cdot(n_{\rm II}\boldsymbol{u}_{\rm II})=0, \tag{4}$$

$$\frac{\partial p_{\rm II}}{\partial t}+\boldsymbol{u}_{\rm II}\cdot\nabla p_{\rm II}+\gamma p_{\rm II}\nabla\cdot\boldsymbol{u}_{\rm II}=0, \tag{5}$$

$$\frac{\partial \boldsymbol{u}_{\rm II}}{\partial t}+\boldsymbol{u}_{\rm II}\cdot\nabla\boldsymbol{u}_{\rm II}+\frac{1}{n_{\rm II}m_{\rm II}}\nabla p_{\rm II}-\frac{1}{4\pi n_{\rm II}m_{\rm II}}(\nabla\times\boldsymbol{B})\times\boldsymbol{B}-\boldsymbol{g}=\nu(\boldsymbol{u}_{\rm I}-\boldsymbol{u}_{\rm II}), \tag{6}$$

$$\frac{\partial \boldsymbol{B}}{\partial t}=\nabla\times(\boldsymbol{u}_{\rm II}\times\boldsymbol{B}), \tag{7}$$

where subscripts I and II specify neutral and ionized fluids, respectively, n is the particle number density, m is the particle mass, u is the velocity, p is the pressure, B is the magnetic field, ν is the collision frequency be-

**Corresponding author. Email: jyjsdl@mail.ustc.edu.cn

© 2018 Chinese Physical Society and IOP Publishing Ltd

tween two species, γ is the polytropic exponent, and g is the gravity.

We make a plane wave decomposition for each of the perturbed quantities as

$$\Psi(\boldsymbol{x},t) = \Psi_0 e^{i(k\boldsymbol{x}-\omega t)}, \tag{8}$$

where Ψ is the amplitude of the plane wave propagating along the $\boldsymbol{x}$ direction, and subscript 0 represents the undisturbed quantities. Moreover, assuming that the unperturbed plasma is static and homogeneous, we can obtain the corresponding wave dispersion relation

$$\begin{aligned}0 = D(\omega,k) =& \omega^3[(\omega+i\nu)(\omega^2-k^2v_{\rm An}^2)+i\nu\omega^2]\\ &\times[\omega^7+4i\nu\omega^6-\omega^5(4\nu^2+2k^2c_{\rm s}^2+k^2v_{\rm A}^2)\\ &+\omega^3k^2(k^2c_{\rm s}^4+k^2c_{\rm s}^2v_{\rm An}^2+k^2c_{\rm s}^2v_{\rm A}^2+4\nu^2c_{\rm s}^2\\ &+2\nu^2v_{\rm A}^2)-3i\nu\omega^4k^2(2c_{\rm s}^2+v_{\rm A}^2)+2i\nu\omega^2k^4(c_{\rm s}^4\\ &+c_{\rm s}^2v_{\rm An}^2+c_{\rm s}^2v_{\rm A}^2)-\omega k^4c_{\rm s}^2v_{\rm An}^2(2\nu^2\\ &+k^2c_{\rm s}^2)-i\nu k^6c_{\rm s}^4v_{\rm An}^2],\end{aligned} \tag{9}$$

where $c_{\rm s}=\sqrt{\gamma RT_0}$ is the sound characteristic (we assume that two species have the same thermal properties with identical undisturbed temperature T_0), R is the gas constant, $v_{\rm A}=\sqrt{\frac{B_0^2}{4\pi m_{\rm I\!I} n_{\rm I\!I0}}}$ is the velocity of Alfven wave propagating parallel to the magnetic field in ionized gas, and $v_{\rm An}=v_{\rm A}\cos\theta$ with the wave normal angle θ. Under the condition of $\nu=0$, the dispersion relation Eq. (9) degenerates to

$$\begin{aligned}0 =& \omega^5(\omega^2-k^2c_{\rm s}^2)\times(\omega^2-k^2v_{\rm An}^2)\\ &\times[\omega^4-\omega^2k^2(c_{\rm s}^2+v_{\rm A}^2)+k^4c_{\rm s}^2v_{\rm An}^2].\end{aligned} \tag{10}$$

For non-trivial solutions, the dispersion relation can be divided into two subset equations: the neural fluid equation

$$0=\omega^2-k^2c_{\rm s}^2, \tag{11}$$

and the ideal MHD equation

$$\begin{aligned}0 =& (\omega^2-k^2v_{\rm An}^2)\\ &\times[\omega^4-\omega^2k^2(c_{\rm s}^2+v_{\rm A}^2)+k^4c_{\rm s}^2v_{\rm An}^2].\end{aligned} \tag{12}$$

Introducing the dimensionless parameters $\bar{\omega}=\omega/\nu$, $\bar{k}=kc_{\rm s}/\nu$ and $s=v_{\rm A}^2/c_{\rm s}^2$ into Eq. (9) yields

$$\begin{aligned}0 = D(\bar{\omega},\bar{k}) =& \bar{\omega}^3[(\bar{\omega}+i)(\bar{\omega}^2-\bar{k}^2s\cos^2\theta)+i\bar{\omega}^2]\\ &\times\{\bar{\omega}^7+4i\bar{\omega}^6-\bar{\omega}^5[\bar{k}^2(s+2)+4]\\ &-3i\bar{\omega}^4\bar{k}^2(s+2)+\bar{\omega}^3\bar{k}^2[\bar{k}^2+\bar{k}^2s\cos^2\theta\\ &+\bar{k}^2s+2(s+2)]+2i\bar{\omega}^2\bar{k}^4(s\cos^2\theta+s+1)\\ &-\bar{\omega}\bar{k}^4s\cos^2\theta(\bar{k}^2+2)-i\bar{k}^6s\cos^2\theta\},\end{aligned} \tag{13}$$

which can be divided into two subset equations for non-trivial solutions

$$0=D_1(\bar{\omega},\bar{k})=(\bar{\omega}+i)(\bar{\omega}^2-\bar{k}^2s\cos^2\theta)+i\bar{\omega}^2, \tag{14}$$

and

$$\begin{aligned}0 =& D_2(\bar{\omega},\bar{k})=\bar{\omega}^7+4i\bar{\omega}^6-\bar{\omega}^5[\bar{k}^2(s+2)+4]\\ &-3i\bar{\omega}^4\bar{k}^2(s+2)+2i\bar{\omega}^2\bar{k}^4(s\cos^2\theta+s+1)\\ &+\bar{\omega}^3\bar{k}^2[\bar{k}^2+\bar{k}^2s\cos^2\theta+\bar{k}^2s+2(s+2)]\\ &-\bar{\omega}\bar{k}^4s\cos^2\theta(\bar{k}^2+2)-i\bar{k}^6s\cos^2\theta.\end{aligned} \tag{15}$$

For a complex wave frequency $\bar{\omega}=\bar{\omega}_r+i\bar{\omega}_{\rm i}$, the analytical solution to Eq. (14) can be expressed as

$$\bar{\omega}_r=\sqrt{3}[t^2+(\bar{k}^2s\cos^2\theta)/12-1/9]/t, \tag{16}$$

$$\bar{\omega}_{\rm i}=t-[(\bar{k}^2s\cos^2\theta)/12-1/9]/t-2/3, \tag{17}$$

where t is denoted by

$$\begin{aligned}t =& \{\{[(\bar{k}^2s\cos^2\theta)/12-1/9]^3+[(\bar{k}^2s\cos^2\theta)/48\\ &+1/27]^2\}^{1/2}+(\bar{k}^2s\cos^2\theta)/48+1/27\}^{1/3}.\end{aligned}$$

This solution corresponds to the Alfven wave mode.

Equation (15) has no general analytical solution. When $\theta=0^\circ$, Eq. (15) can be simplified to

$$\begin{aligned}0 = D_2(\bar{\omega},\bar{k}) =& (\bar{\omega}^2-\bar{k}^2)(\bar{\omega}^2-\bar{k}^2+2i\bar{\omega})\\ &\times[(\bar{\omega}+i)(\bar{\omega}^2-\bar{k}^2s)+i\bar{\omega}^2].\end{aligned} \tag{18}$$

There are three non-trivial solutions to Eq. (18): the sound wave

$$\bar{\omega}=\bar{k}, \tag{19}$$

the slow magnetoacoustic wave

$$\bar{\omega}=\sqrt{\bar{k}^2-1}-i,\ \bar{k}>1, \tag{20}$$

and the fast magnetoacoustic wave which has degenerated into the Alfven wave (Eqs. (16) and (17)). When $\theta=90^\circ$, Eq. (15) can be simplified with the complex wave frequency as

$$\begin{aligned}0 = D_2(\bar{\omega},\bar{k}) =& (\bar{\omega}_r+i\bar{\omega}_{\rm i})^2(\bar{\omega}_r+i\bar{\omega}_{\rm i}+2i)\\ &\times\{\{\bar{\omega}_r^4-\bar{\omega}_r^2[6\bar{\omega}_{\rm i}^2+6\bar{\omega}_{\rm i}+\bar{k}^2(s+2)]\\ &+\bar{\omega}_{\rm i}^4+2\bar{\omega}_{\rm i}^3+\bar{\omega}_{\rm i}\bar{k}^2(\bar{\omega}_{\rm i}+1)(s+2)\\ &+\bar{k}^4(s+1)\}+i\bar{\omega}_r[2\bar{\omega}_r^2(2\bar{\omega}_{\rm i}+1)\\ &-4\bar{\omega}_{\rm i}^3-6\bar{\omega}_{\rm i}^2-\bar{k}^2(2\bar{\omega}_{\rm i}+1)(s+2)]\}.\end{aligned} \tag{21}$$

The corresponding analytical solutions can be expressed as

$$\bar{\omega}_r^2=[4\bar{\omega}_{\rm i}^3+6\bar{\omega}_{\rm i}^2+\bar{k}^2(2\bar{\omega}_{\rm i}+1)(s+2)]/(4\bar{\omega}_{\rm i}+2), \tag{22}$$

$$\bar{\omega}_{\rm i}=\pm\sqrt{u}-0.5, \tag{23}$$

with

$$\begin{aligned}u =& (2^{1/3}/24)[2^{1/3}t^2+2^{2/3}(3-2\bar{k}^2s-4\bar{k}^2)t\\ &+2\bar{k}^4s^2+32\bar{k}^4s-12\bar{k}^2s+32\bar{k}^4-24\bar{k}^2]/t,\\ t =& \{3\sqrt{3}[\bar{k}^6(4\bar{k}^4s^5-16\bar{k}^6s^4-16\bar{k}^6s^5+72\bar{k}^4s^4\\ &+192\bar{k}^4s^3+128\bar{k}^4s^2-13\bar{k}^2s^4-224\bar{k}^2s^3\\ &-480\bar{k}^2s^2-512\bar{k}^2s-256\bar{k}^2+32s^3+192s^2\\ &+384s+256)]^{1/2}+144\bar{k}^4s-192\bar{k}^6s+144\bar{k}^4\\ &-128\bar{k}^6+9\bar{k}^4s^2-60\bar{k}^6s^2+2\bar{k}^6s^3\}^{1/3}.\end{aligned}$$

For perpendicular propagation, these solutions are the fast magnetoacoustic wave and the sound wave.

The dispersion relations of all these waves-modes under different conditions of s and θ are plotted in Fig. 1. One can find that all the wave phase velocities from the two-fluid model are almost the same as those from the collisionless model. The imaginary part $\bar{\omega}_{\rm i}$ of wave frequency is negative, indicating that these waves will be damped by the collision between two species. As $\bar{k}$ increases, $\bar{\omega}_{\rm i}$ will asymptotically reach a value. For the fast magnetoacoustic and Alfven waves, the asymptotic values of $\bar{\omega}_{\rm i}$ are -0.5, independent of the wave normal angle. For the slow magnetoacoustic wave, the asymptotic value of $\bar{\omega}_{\rm i}$ is -1 when $\theta = 0^\circ$ but becomes -0.5 for other normal angles. For the sound wave, the asymptotic value of $\bar{\omega}_{\rm i}$ reaches 0 but decreases to -0.5 at other normal angles.

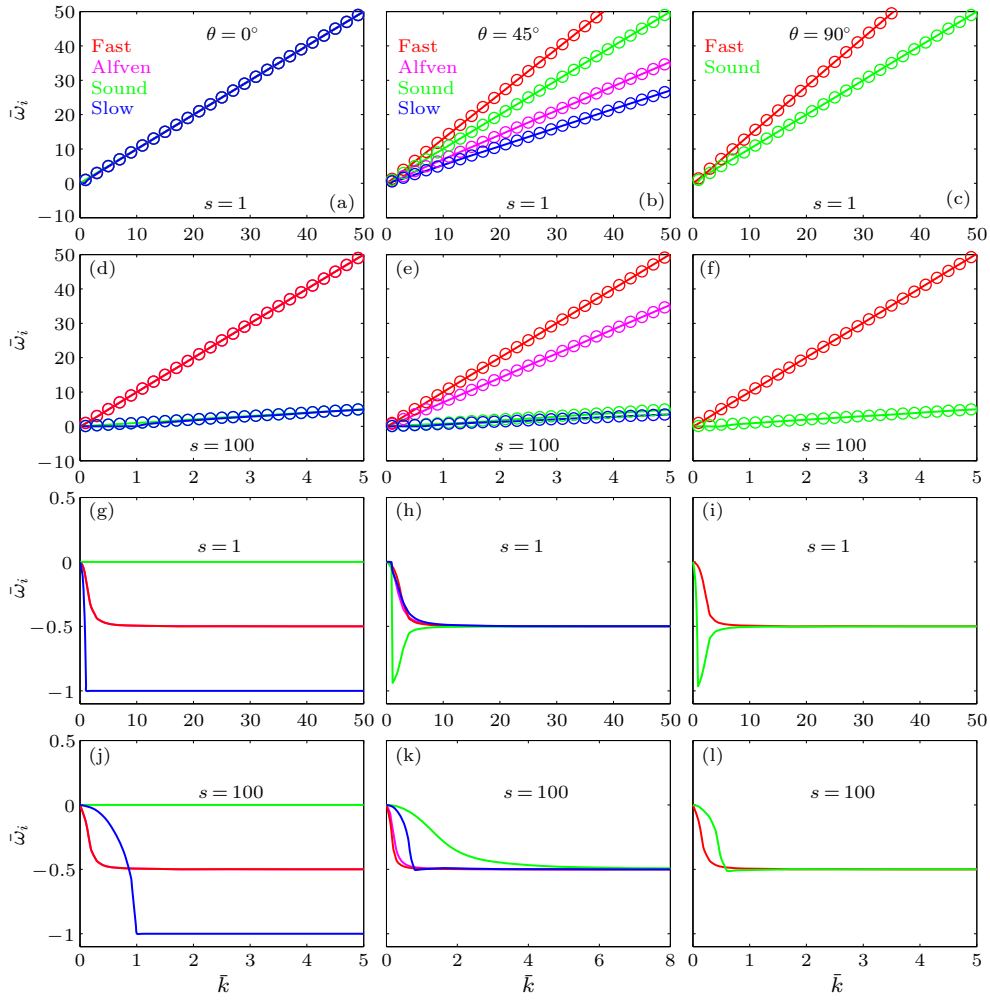

Fig. 1. The real part solutions ((a)–(f)) and the imaginary part solutions ((g)–(l)) of the dispersion relation under different conditions of s and θ, with lines for the collision model and circles for the collisionless model. Colors help differentiate among the wave modes.

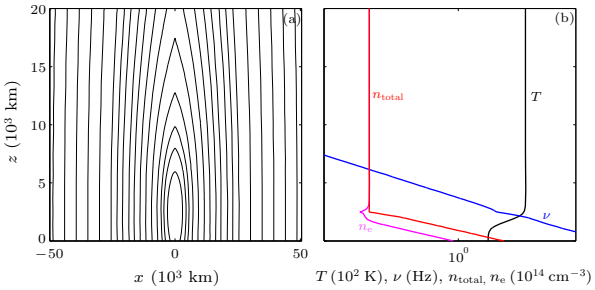

Fig. 2. (a) Magnetic field configuration. (b) Height-dependence of temperature, collision frequency, overall and ionized densities.

For better exploring the characteristics of the Moreton waves and EUV waves, the modeled magnetic field, temperature, collision frequency, as well as the overall and ionized gas densities are plotted in Fig. 2. EUV waves are mostly generated by a flux-rope eruption at the early stage of CME, thus the source region magnetic field is assumed to be[14]

$$B_y(r) = \sqrt{B_{y0}^2\left(1 - \frac{r^2}{r_{\rm e}^2}\right)}, \quad r \leqslant r_{\rm e}$$

$$B_y(r) = 0, \quad r > r_{\rm e} \tag{24}$$

$$B_r(r) = B_{\rm ze} \sin\phi, \tag{25}$$

$$B_\phi(r) = \frac{B_{\phi e}}{2}[\sin(\frac{\pi r}{r_e} - \frac{\pi}{2}) + 1] + B_{ze}\cos\phi,\ r \leqslant r_e$$
$$B_\phi(r) = B_{\phi e} r_e/r + B_{ze}\cos\phi,\ r > r_e, \quad (26)$$
$$r^2 = x^2 + (z - z_0)^2. \quad (27)$$

This magnetic field configuration consists of a flux rope centered at $(x = 0, z = z_0)$, overlying field, and the background open field. The location and size of the flux rope are specified as $z_0 = 2000$ km and $r_e = 1000$ km. The magnetic field strength of the flux rope is determined by $B_{y0} = 20$ G, $B_{\phi e} = 20$ G and $B_{ze} = 1$ G. The temperature and the ionization rate are modeled as[36,37]

$$T = \frac{1}{2}(T_{cor} + T_b) + \frac{1}{2}(T_{cor} - T_b)\tanh\left(\frac{z - z_t}{z_s}\right), \quad (28)$$
$$\log_{10}\alpha = \frac{1}{2}(\log_{10}\alpha_{cor} + \log_{10}\alpha_b) + \frac{1}{2}(\log_{10}\alpha_{cor} - \log_{10}\alpha_b)\tanh\left(\frac{z - z_t}{z_s}\right), \quad (29)$$

where $T_{cor} = 10^6$ K and $T_b = 10^4$ K are the temperatures in the corona and chromosphere, $\alpha_{cor} = 1$ and $\alpha_b = 0.001$ are the ionization ratio in the corona and chromosphere, respectively, $z_t = 2200$ km is the location of the maximum gradient in the transition region, and $z_s = 400$ km is the length scale. The used parameters are selected according to the quiet-atmosphere model.[36] We use a linear height-dependence total particle number density model,[14] with a base density of 5×10^{16} cm^{-3} and a coronal density of 5×10^8 cm^{-3}.[36] Because the ion-neutral collision frequency is far lower than the electron-neutral collision frequency, we only take into account the electron-neutral collision here. The collision frequency ν is set as[38]

$$\nu = n_n u_e \sigma_{en}, \quad (30)$$

where n_n is the neutral gas density deduced from Eqs. (28) and the particle number density n, $\sigma_{en} = 10^{-15}$ cm^2 is the electron-neutral collisional cross section,[38] and $u_e = \sqrt{\frac{2k_bT_e}{m_e}}$ is the electron thermal velocity.

With the above models, the velocity and damping rate of the corresponding fast magnetoacoustic waves are plotted in Fig. 3. We next calculate the propagation and damping of a fast magnetoacoustic wave based on the following equations

$$\frac{dx}{dt} = u(x), \quad (31)$$
$$\frac{d\ln A(x,t)}{dt} = \omega_i(x), \quad (32)$$

where u is the velocity along the x direction, ω_i is the imaginary part of the wave frequency, and A is the wave amplitude. Note that the wave refraction and dispersion have been ignored. In the calculation, the wave angular frequency is specified as 100 rad·s^{-1}. As shown in Fig. 4, we trace the wave fronts initialized at two typical heights of 2000 and 5500 km.

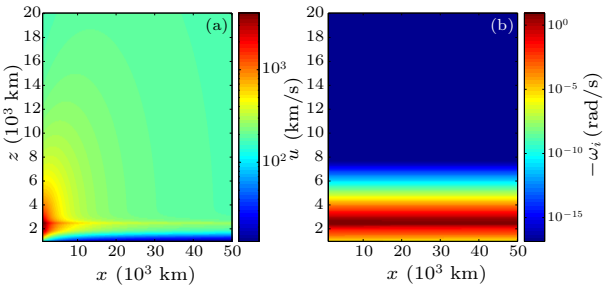

Fig. 3. Spatial distributions of (a) velocity and (b) damping rate of the fast magnetoacoustic wave in the solar atmosphere. The velocity is along the $\boldsymbol{x}$ direction.

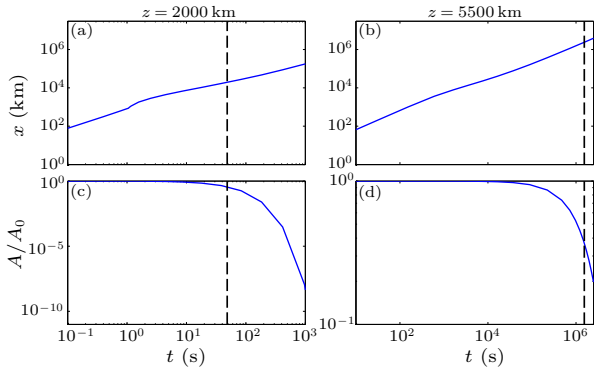

Fig. 4. Temporal evolution of ((a), (b)) wave fronts and ((c), (d)) amplitude decay ratios of the fast magnetoacoustic waves at different heights. Here A_0 is the initial amplitude and the dashed lines mark the time points at which the amplitudes decrease to A_0/e.

Near the source region ($x < 6000$ km), the chromosphere has a stronger magnetic field and a lower ionization rate than the corona. Correspondingly, the wave velocity (550–2500 km·s^{-1} at 2000 km) in the chromosphere is much higher than that (350–550 km·s^{-1} at 5500 km) in the corona. Note that the fast mode velocity produced from the one-fluid model is only a few tens of km/s in the chromosphere, but the velocity from the two-fluid model (using the partially ionized plasma density) can match the Moreton wave velocity well. As the waves propagate away from the source region, the velocity changes slightly in the corona but slows down very quickly in the chromosphere, consistent with the previous observations.[4] At $z > 6000$ km with the almost fully ionized plasma, the damping is very weak. In contrast, the damping rate ranges from 10^{-5}–10^0 rad·s^{-1} at $z < 4000$ km with the partially ionized plasma. Hence, the waves in the chromosphere have a much shorter lifetime (1 min at 2000 km) than those (4 h at 5500 km) in the corona. In other words, the EUV wave is observable over a longer distance than the Moreton wave. These results qualitatively explain the observed difference of velocities and lifetimes between the Moreton and EUV waves.[4,5,8,19,20]

In summary, we here analyzed the wave character-

istics of a two-fluid MHD model in the stratified solar atmosphere with a height-dependent ionization rate. The collisions between neutral and ionized fluids are found to affect insignificantly the wave velocities but attenuate obviously the wave amplitudes. Compared with the chromosphere, the corona has the higher ionization rate and the weaker magnetic fields. Consequently, the EUV wave propagates more slowly than the Moreton wave. In the chromosphere, the collision between neutral and ionized fluids leads to the damping of the Moreton waves on a timescale of a few minutes. On the contrary, in the fully ionized corona, the EUV wave is able to propagate globally on a time scale of several hours. Our results support that fast MHD waves account for both EUV and the Moreteon waves in the different layers of the solar atmosphere. Furthermore, the solar lower atmosphere is a highly dynamic nonequilibrium plasma, existing with the non-ionizing equilibrium effect, charge exchange, Hall effect, radiation cooling, heat conduction and ion viscosity.[7] The magnetic field in the solar lower atmosphere is a multipolar field with complex topology,[39] there may exist magnetic zero and separation planes at low heliocentric height. Hence, a further in-depth study, with consideration of one or more factors mentioned above, may reveal more realistic EUV wave observation characteristics.

References

[1] Plunkett S P, Thompson B J, Howard R A, Michels D J, St O C, Tappin S J, Schwenn R and Lamy P L 1998 *Geophys. Res. Lett.* **25** 2477
[2] Thompson B J, Plunkett S P, Gurman J B, Newmark J S, St O C and Michels D J 1998 *Geophys. Res. Lett.* **25** 2465
[3] Thompson B J and Myers D C 2009 *Astrophys. J. Suppl. Ser.* **183** 225
[4] Muhr N, Veronig A M, Kienreich I W, Vršnak B, Temmer M and Bein B M 2014 *Sol. Phys.* **289** 4563
[5] Long D M, Bloomfield D S, Chen P F, Downs C, Gallagher P T, Kwon R Y, Vanninathan K, Veronig A M, Vourlidas A, Vršnak B, Warmuth A and Žic T 2017 *Sol. Phys.* **292** 7
[6] West M J, Zhukov A N, Dolla L and Rodriguez L 2011 *Astrophys. J.* **730** 122
[7] Cally P S and Xiong M 2018 *J. Phys.* A **51** 025501
[8] Warmuth A 2015 *Living Rev. Sol. Phys.* **12** 3
[9] Chen P F 2017 *Sci. Chin.-Phys. Mech. Astron.* **60** 029631
[10] Delannée C and Aulanier G 1999 *Sol. Phys.* **190** 107
[11] Chen P F, Wu S T, Shibata K and Fang C 2002 *Astrophys. J.* **572** L99
[12] Chen P F 2009 *Astrophys. J.* **698** L112
[13] Uchida Y 1968 *Sol. Phys.* **4** 30
[14] Vršnak B, Žic T, Lulić S, Temmer M and Veronig A M 2016 *Sol. Phys.* **291** 89
[15] Wang Y M 2000 *Astrophys. J.* **543** L89
[16] Downs C, Roussev I I, van der Holst B, Lugaz N, Sokolov I V and Gombosi T I 2011 *Astrophys. J.* **728** 2
[17] Downs C, Roussev I I, van der Holst B, Lugaz N and Sokolov I V 2012 *Astrophys. J.* **750** 134
[18] Kwon R Y, Ofman L, Olmedo O, Kramar M, Davila J M, Thompson B J and Cho K S 2013 *Astrophys. J.* **766** 55
[19] Warmuth A, Vršnak B, Aurass H and Hanslmeier A 2001 *Astrophys. J.* **560** L105
[20] Warmuth A, Vršnak B, Magdalenić J, Hanslmeier A and Otruba W 2004 *Astron. Astrophys.* **418** 1101
[21] Warmuth A, Vršnak B, Magdalenić J, Hanslmeier A and Otruba W 2004 *Astron. Astrophys.* **418** 1117
[22] Zheng H N, Zhang Y Y, Wang S, Wang C B and Li Y 2006 *Chin. Phys. Lett.* **23** 399
[23] Gopalswamy N, Yashiro S, Temmer M, Davila J, Thompson W T, Jones S, McAteer R T J, Wuelser J P, Freel S and Howard R A 2009 *Astrophys. J. Lett.* **691** L123
[24] Asai A, Ishii T T, Isobe H, Kitai R, Ichimoto K, Ueno S, Nagata S, Morita S, Nishida K, Shiota D, Oi A, Akioka M and Shibata K 2012 *Astrophys. J. Lett.* **745** L18
[25] Olmedo O, Vourlidas A, Zhang J and Cheng X 2012 *Astrophys. J.* **756** 143
[26] Muhr N, Vršnak B, Temmer M, Veronig A M and Magdalenić J 2010 *Astrophys. J.* **708** 1639
[27] Liu R, Liu C, Xu Y, Liu W, Kliem B and Wang H 2013 *Astrophys. J.* **773** 166
[28] Wills-Davey M J, DeForest C E and Stenflo J O 2007 *Astrophys. J.* **664** 556
[29] Wang H, Shen C and Lin J 2009 *Astrophys. J.* **700** 1716
[30] Patsourakos S and Vourlidas A 2012 *Sol. Phys.* **281** 187
[31] Liu W and Ofman L 2014 *Sol. Phys.* **289** 3233
[32] Stein R F and Leibacher J 1974 *Annu. Rev. Astron. Astrophys.* **12** 407
[33] Lenz D D 1999 *Astrophys. J.* **517** 497
[34] Schunk R W 1975 *Planet. Space Sci.* **23** 437
[35] Judge P G and Peter H 1998 *Space Sci. Rev.* **85** 187
[36] Vernazza J E, Avrett E H and Loeser R 1981 *Astrophys. J.* **45** 635
[37] Cargill P J, Spicer D S and Zalesak S T 1997 *Astrophys. J.* **488** 854
[38] Khodachenko M L, Arber T D, Rucker H O and Hanslmeier A 2004 *Astron. Astrophys.* **422** 1073
[39] Bravo S, Stewart G A and Blanco-Cano X 1998 *Sol. Phys.* **179** 223